The origin of photovoltaic responses in BiFeO3 multiferroic ceramics

Authors: C.-S. Tu, C.-M. Hung, V. Hugo Schmidt, R. R. Chien, M.-D. Jiang, and J. Anthoninappen

C.-S. Tu, C.-M. Hung, V.H. Schmidt, R.R. Chien, M.-D. Jiang, and J. Anthoninappen, “The origin of photovoltaic responses in BiFeO3 multiferroic ceramics,” Journal of Physics: Condensed Matter 24, 495902 (5 pp.) (2012). doi: 10.1088/0953-8984/24/49/495902.

The origin of photovoltaic responses in $BiFeO_3$ multiferroic ceramics

C-S Tu[1,2], C-M Hung[1], V H Schmidt[3], R R Chien[3], M-D Jiang[2] and J Anthoninappen[1]

[1] Graduate Institute of Applied Science and Engineering, Fu Jen Catholic University, Taipei 24205, Taiwan

[2] Department of Physics, Fu Jen Catholic University, Taipei 24205, Taiwan

[3] Department of Physics, Montana State University, Bozeman, MT 59717, USA

Abstract

Multiferroic $BiFeO_3$ (BFO) ceramics with electrodes of indium tin oxide (ITO) and Au thin films exhibit significant photovoltaic effects under near-ultraviolet illumination ($\lambda = 405$ nm) and show strong dependences on light wavelength, illumination intensity, and sample thickness. The correlation between photovoltaic responses and illumination intensity can be attributed to photo-excited and thermally generated charge carriers in the interface depletion region between BFO ceramic and ITO thin film. A theoretical model is developed to describe the open-circuit photovoltage and short-circuit photocurrent density as a function of illumination intensity. This model can be applied to the photovoltaic effects in p–n junction type BFO thin films and other systems. The BFO ceramic exhibits stronger photovoltaic responses than the ferroelectric $Pb_{1-x}La_x(Zr_yTi_{1-y})_{1-x/4}O_3$ (PLZT) ceramics under near-ultraviolet illumination. Comparisons are made with other systems and models for the photovoltaic effect.

(Some figures may appear in colour only in the online journal)

1. Introduction

Photovoltaic and photostrictive effects have been extensively investigated in antiferromagnetic/ferroelectric $BiFeO_3$ (BFO) thin films a nd c rystals [1–13]. S everal m echanisms were proposed for the photovoltaic responses in BFO thin films and crystals, including asymmetric ferroelectric photovoltaic effect (bulk photovoltaic effect) [7, 14], domain-wall model [8], and semiconductor-like p–n junction model [13]. The domain walls in rhombohedral BFO thin films exhibit a p–n junction-like potential step, whose value is theoretically higher in the 109° domain walls (∼0.15 V) compared to the 71° domain walls (∼0.02 V) [9]. The effects of electric (E)-field poling [2], illumination wavelength and intensity [2, 5], substrate [4], and electrode [5, 6] on photovoltaic responses and optical properties of BFO films have also been explored. In addition, the photostrictive effect in BFO crystal can reach 10^{-5} with response time less than 0.1 s, which depends on light polarization and magnetic field [11].

A p-type semiconductivity was found in BFO film with impurity density of $n_p \sim 10^{23}$ m^{-3} [13]. The photovoltaic responses were attributed to a p–n junction layer at the ITO–BFO interface. ITO film has been reported as being a n-type semiconductor with carrier concentration of $n_n \sim 10^{26}$–10^{27} m^{-3} [15, 16]. Photovoltaic responses were also observed in the p–n depletion layer of a $LaMnO_3$/Nb-doped $SrTiO_3$ structure, in which $LaMnO_3$ plays the role of p-type semiconductor [17]. The photovoltaic responses of ferroelectric/piezoelectric PLZT ceramics and $Pb(Mg_{1/3}Nb_{2/3})_{1-x}Ti_xO_3$ (PMN–PT) crystals are sensitive to thickness and grain size [18–21]. A photovoltaic mechanism associated with charge distributions (polarization charge, Schottky space charge, and screening charge) was proposed for PLZT thin films and its efficiency can be improved with reduced thickness [22].

Most photovoltaic studies and proposed mechanisms in BFO films have been focusing on the current–voltage correlation under a constant light intensity. In this work,

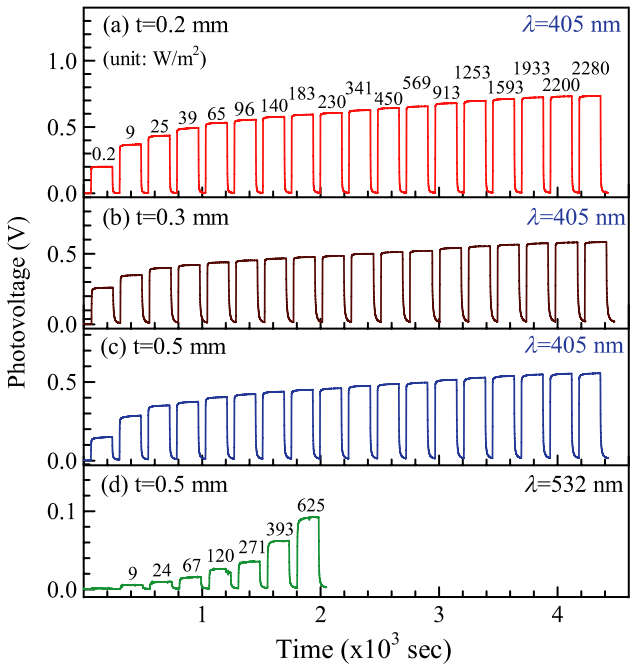

Figure 1. Open-circuit photovoltage (V_{oc}) as light was switched on and off with increasing light intensity. The intensity is labeled on the top of each illumination.

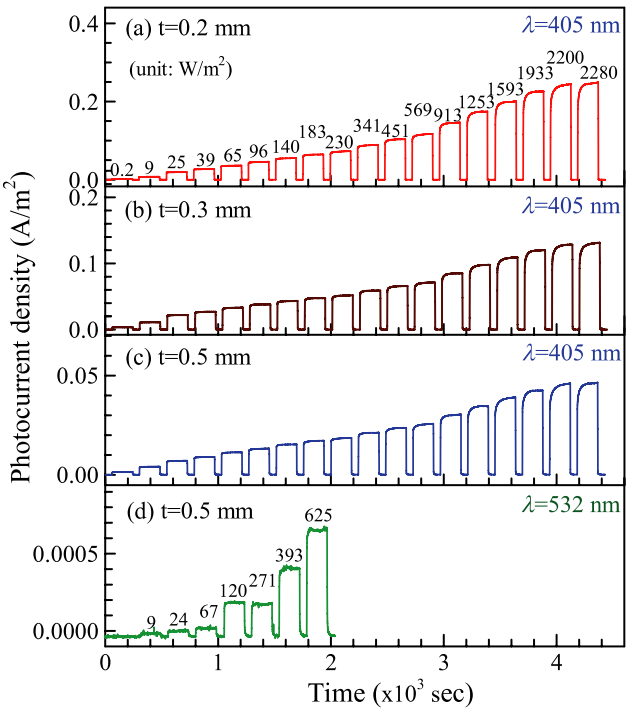

Figure 2. Short-circuit photocurrent density (J_{sc}) with increasing light intensity.

a theoretical model was first proposed to describe the correlation between photovoltaic responses and illumination intensity in the ITO film/BFO ceramics/Au film capacitor configuration.

2. Experimental details

The $BiFeO_3$ (BFO) ceramics were prepared by the solid state reaction method. In the synthesis, Bi_2O_3 and Fe_2O_3 powders (purity $\geq$ 99.0%) were weighed in 1.1:1 ratio to compensate the loss of Bi during the sintering process. The powders were mixed in an agate mortar for more than 24 h using alcohol as a medium. The mixture was dried before calcining at 800 °C for 3 h. The calcined powder was then pressed into a disk before sintering at 830 °C for 10 h. ITO and Au films were deposited on the BFO ceramic as electrodes by dc sputtering. Two intensity-adjustable diode lasers of $\lambda = 405$ and 532 nm were used for photovoltaic effects. The laser beam was incident perpendicular to the sample surface with ITO film.

3. Results and discussion

Figures 1 and 2 show open-circuit photovoltage (V_{oc}) and short-circuit photocurrent density (J_{sc}) as light was switched on and off under illuminations of $\lambda = 405$ and 532 nm for thicknesses of $t = 0.2$, 0.3, and 0.5 mm. Both V_{oc} and J_{sc} exhibits strong and nonlinear dependences on light intensity (I) and wavelength (λ). The intensity-dependent V_{oc} and J_{sc} are plotted in figures 3 and 4. Compared with $\lambda = 532$ nm, the illumination of $\lambda = 405$ nm ($E_{ph} \sim 3.06$ eV) induces much stronger photovoltaic responses. These results agree with the optical band gap of ~2.74 eV in BFO [2, 12]. The J_{sc} for $t = 0.2$ mm can reach ~0.23 A m^{-2} for $I \sim 1.9 \times 10^3$ W m^{-2} under illumination of $\lambda = 405$ nm. This J_{sc} is much stronger than in the poled PLZT(3/52/48) ceramics, whose J_{sc} ($t = 50\ \mu$m) shows a linear increase with I and is ~0.2 mA m^{-2} for $I \sim 2 \times 10^3$ W m^{-2} under illumination of $\lambda = 366$ nm [18].

To understand the light intensity-dependent V_{oc} and J_{sc}, a theoretical model is derived as follows. We consider a p-type BFO slab on the right and an n-type ITO slab on the left. Electrons will diffuse right, and holes diffuse left, annihilating each other and leaving a depletion region. The first task is to find the open-circuit voltage step $-U_o$ going from left to right across the p–n junction under no illumination. For no illumination, this voltage is cancelled by a voltage U_o from the contacts to the ITO and BFO. In the depletion region, there will be a small thermally generated electron–hole creation rate, and in this region the holes will go right and the electrons left, giving a small current to the right. For no illumination there can be no net current. The compensating current is from holes from the non-depleted p-type BFO diffusing 'uphill' in electrostatic energy to the non-depleted n-type ITO and from electrons from the non-depleted n-type ITO diffusing 'uphill' in electrostatic energy to the non-depleted BFO.

In addition to the thermally generated charges, many electron–hole pairs will be generated optically under illumination. These additional holes will flow right, and the electrons left, thereby decreasing the depletion-region width. However, the decreased width will lower the retarding voltage that limits the leftward hole and electron diffusion currents, thus increasing these currents. The decreased width decreases the downward voltage step from the depletion region, to magnitude $U < U_o$, and so the measured open-circuit

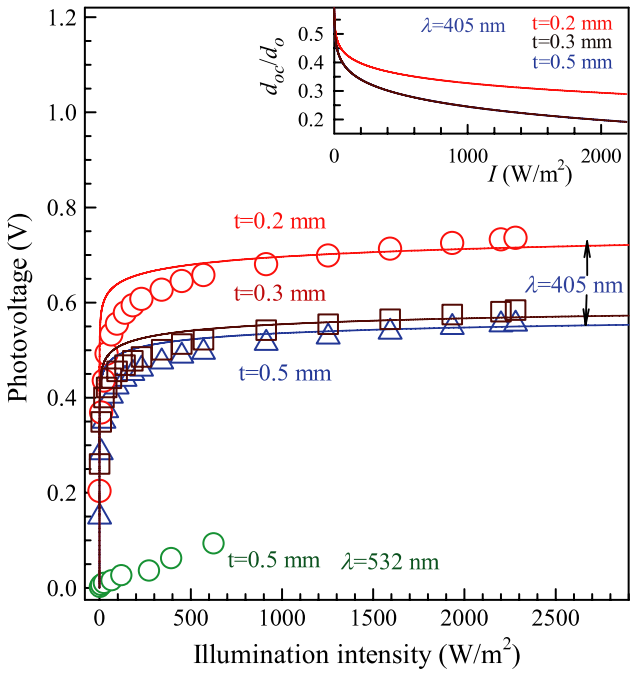

Figure 3. The experimental open-circuit photovoltage and theoretical fits versus intensity. The inset is the ratio d_{oc}/d_o (=D_{oc}) as a function of light intensity for λ = 405 nm.

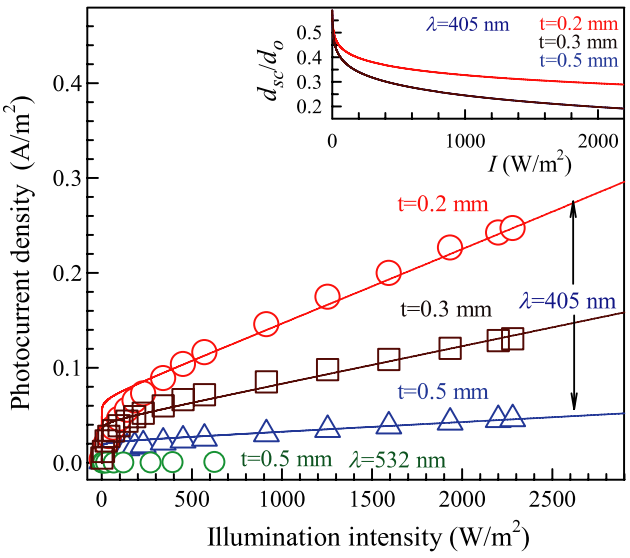

Figure 4. The experimental short-circuit photocurrent density and theoretical fits versus intensity. The inset is the ratio d_{sc}/d_o (=D_{sc}) as a function of light intensity for λ = 405 nm.

voltage is

$$V_{oc}(I) = U_o - U_{oc}(I). \tag{1}$$

There are three contributions to the total current density J. The first contribution J_t is from thermally stimulated electron–hole pairs created in the depletion region. The number density n_v of electrons close enough to the top of the valence band so that they have a chance to be excited to the conduction band is assumed to be $n_v = NkT/E_{vn}$, where N is the density of electrons in the valence band, k is Boltzmann's constant, $T = 300$ K is chosen as room temperature, and E_{vn} is the top energy of the valence band. The thermal excitation probability p_v per unit time per electron is $p_v = v\exp(-E_{cn}/kT)$, where v is the attempt frequency and E_{cn} is the bottom energy in the conduction band. Considering both the n- and p-type regions, we multiply $n_v p_v$ by the depletion-region width d and by the carrier charge q to find J_t,

$$J_t = qkTv[(d_n N_n/E_{vn})e^{-E_{cn}/kT} + (d_p N_p/E_{vp})e^{-E_{cp}/kT}]. \tag{2}$$

The second contribution to J is the J_e from existing carriers that are close to the depletion region and have enough thermal energy to jump across it against the coulomb force. The dopant concentration n is assumed to be independent of position. The holes (or electrons) that are close enough to the depletion region so that when thermally excited they do not lose much energy to other carriers, are assumed to come from a plane of thickness corresponding to the mean spacing between acceptors (or donors). The number density per unit area of these potentially excited carriers accordingly is $n_p^{2/3}$ (or $n_n^{2/3}$). The probability per unit time per carrier that such a carrier obtains enough energy to cross the depletion region is $v\exp(-qU/kT)$. The hole and electron contributions to J_e are negative, so J_e is given by

$$J_e = -qv(n_n^{2/3} + n_p^{2/3})e^{-qU/kT}. \tag{3}$$

The third contribution is the photo-excited current density J_p. The light intensity is assumed to decay exponential in the BFO-side depletion region with a general form of $I(z) = I\exp(-z/\beta)$, where β is the attenuation length. The ITO layer absorbs little light because its optical band gap is larger than the photon energy. The absorbed intensity I_a in the depletion region can be estimated by $I_a = Id/\beta$. The creation rate of electron–hole pairs can be estimated to be $I_a/(hc/\lambda)$, then J_p is given by

$$J_p = qdI\lambda/(hc\beta). \tag{4}$$

We now find an expression for the p–n junction voltage step $-U$ in terms of the depletion-region widths d_p and d_n, which are parameters of light intensity. Let position coordinate x be zero at the interface of the p–n junction. In the depletion region of $-d_n < x < 0$, $\rho_n = qn_n$ comes from the ionized donors each of which has donated one electron to the conduction band. Similarly, in the depletion region of $0 < x < d_p$, $\rho_p = qn_p$ comes from the acceptors each of which has accepted one electron from the valence band. Using Gauss' law for the region $-d_n < x < 0$, the position-dependent E-field is,

$$E(x) = \int_{-d_n}^{x} (\rho_n/\varepsilon_o\varepsilon_n)\,dx' = (\rho_n/\varepsilon_o\varepsilon_n)(x + d_n). \tag{5}$$

Then the contribution from the n-type material to $-U$ is,

$$-U_n = -\int_{-d_n}^{0} E(x)\,dx = -(\rho_n/\varepsilon_o\varepsilon_n)d_n^2/2. \tag{6}$$

Table 1. The fitting parameters for the solid lines in figures 3 and 4.

$\lambda = 405$ nm	U_o (V)	C	α (W m^{-2})$^{-1}$	R_{AO} (Ω m^2)	η (W m^{-2})$^{-1}$
$t = 0.2$ mm	0.78	28	2.2×10^8	9.4	0.001
$t = 0.3$ mm	0.59	23	1.0×10^7	12	0.0008
$t = 0.5$ mm	0.57	23	1.0×10^7	23	0.0004

Similarly, $-U_p = (\rho_p/\varepsilon_o\varepsilon_p)d_p^2/2$ is from the p-type material. The total contributions for $-U$ are

$$-U = (\rho_p/\varepsilon_o\varepsilon_p)d_p^2/2 - (\rho_n/\varepsilon_o\varepsilon_n)d_n^2/2$$
$$= (-q/2\varepsilon_o)(n_p d_p^2/\varepsilon_p + n_n d_n^2/\varepsilon_n) \quad (7)$$

ε_p and ε_n are the dielectric permittivities of p- and n-type materials. d_n and d_p are not independent, but are related by the requirement that there is no net charge in the junction region. This requirement gives $d_n = (n_p/n_n)d_p$. We designate d_p as simply d. Then equation (7) yields

$$-U = -(qd^2 n_p/2\varepsilon_o\varepsilon_p)(1 + n_p\varepsilon_p/\varepsilon_n n_n) = -Bd^2;$$
$$B = (qn_p/2\varepsilon_o\varepsilon_p)(1 + n_p\varepsilon_p/\varepsilon_n n_n). \quad (8)$$

We use the condition of no illumination to solve for U_o, and designate d as d_o. For no illumination we have $J_{to} + J_{eo} = 0$, i.e.

$$qkTvd_o[(N_n n_p/n_n E_{vn})e^{-E_{cn}/kT} + (N_p/E_{vp})e^{-E_{cp}/kT}]$$
$$- qv(n_n^{2/3} + n_p^{2/3})e^{-qBd_o^2/kT} = 0. \quad (9)$$

Before solving d_o and U_o, it is worthwhile to know how J_{to} is related to the diode reverse saturation current I_o. We rewrite equation (9), still for no illumination, but now with an applied voltage V_a given by $V_a = U_o - U$. From equation (8), we have $d = [(U_o - V_a)/B]^{1/2}$. Inserting this d value in place of d_o in equation (9) gives the current density J_a resulting from V_a:

$$J_a = J_{to}[(1 - V_a/U_o)^{1/2} - \exp(V_a/V_c)], \quad (10)$$

where $V_c \equiv kT/q$. The diode current–voltage characteristic as given by Shockley *et al* [23] is

$$J_a = (I_0/A)[1 - \exp(V_a/V_c)], \quad (11)$$

where A is junction area. As increasingly negative voltage is applied, the exponential term quickly approaches zero, before the square root term in equation (10) changes appreciably from unity, so J_a becomes J_{to} in equation (10) and I_0/A in equation (11).

Now we use equation (9) to solve d_o. We can use equations (2), (3), and (8) to find U_o, J_{to}, and J_{eo}. To find V_{oc}, we start by finding the d that gives $J_t + J_e + J_p = 0$. Then we find U corresponding to this d, and use $V = U_o - U$. We set $D = d/d_o$, $\alpha = qd_o\lambda/(hc\beta J_{to})$, and $C = qBd_o^2/kT = qU_o/kT$. For the open-circuit case, the illumination intensity-dependent $D_{oc} = d_{oc}/d_o$ can be obtained by

$$J_t + J_p + J_e = J_{to}D_{oc} + J_{to}D_{oc}\alpha I$$
$$- J_{to}\exp[C(1 - D_{oc}^2)] = 0. \quad (12)$$

Then the V_{oc} can be obtained by using equation (8), i.e.

$$V_{oc} = U_o - BD_{oc}^2 d_o^2 = U_o(1 - D_{oc}^2). \quad (13)$$

Now we investigate the total short-circuit current density J_{sc} and area-specific resistance $R_A = RS$, where $R = R_s + R_l$ (source plus load resistance) and S is the illuminated area of the p–n junction. Note that R_l is zero in the short-circuit case. The resistivity of semiconductors typically decreases as temperature is increased. If the temperature due to laser illumination does not vary too much, a linear approximation between resistance and intensity can be used, i.e. $R_A = R_{AO}(1 - \eta I)$. η is the intensity coefficient of resistance. The emf driving the J_{sc} through the source area-specific R_A is $U_o - U_{sc}$. Here, the J_{sc} is,

$$J_{sc} = (U_o - U_{sc})/R_A = U_o(1 - D_{sc}^2)/R_A. \quad (14)$$

From equation (12), modified for the short-circuit case, we have

$$J_{sc} = J_{to}\{D_{sc}(1 + \alpha I) - \exp[C(1 - D_{sc}^2)]\}. \quad (15)$$

We subtract equation (14) from equation (15) and use $F \equiv U_o/R_A J_{to}$. We then obtain

$$D_{sc}(1 + \alpha I) - \exp[C(1 - D_{sc}^2)] - F(1 - D_{sc}^2) = 0. \quad (16)$$

The short-circuit $D_{sc} = d_{sc}/d_o$ as a function of I can be obtained from equation (16). Then, the J_{sc} can then be obtained from equation (15). In the fitting, a weak intensity-dependent resistance was used in F, i.e. $F \cong U_o(1 + \eta I)/R_{AO}J_{to}$.

The solid lines in figures 3 and 4 are fits of V_{oc} and J_{sc} as a function of intensity (I) by using equations (12)–(16) with parameters given in table 1. The experimental results and theoretical fits agree reasonably well. The insets of figures 3 and 4 show the correlation between the ratio d/d_o and light intensity for the open-circuit and short-circuit cases. The measured V_{oc} are comparable with the BFO thin films, whose V_{oc} varies in the range of 0.3–0.5 V [2, 6]. The measured V_{oc} was predicted by our model if values for E_{vn}, E_{vp}, E_{cn} and E_{cp} from the literature are used in equations (8), (9), and (12) to find d_o, d_{oc} and U_o, and then equation (13) is used to find V_{oc}. In fact, our model using these parameters predicts V_{oc} in the 0.3–0.5 V range found in BFO thin-film-based structures as well as in common photovoltaic junction materials like Si and Ge.

In choosing the fit parameters, we note that the carrier concentration n_n in the n-type ITO films is larger than n_p in the p-type BFO films [13, 15, 16]. Thus, from equation (8) we have $B = U_o/d_o^2 \cong qn_p/(2\varepsilon_o\varepsilon_p)$. The room-temperature dielectric permittivity ε_p in BFO ceramic is $\sim 10^2$ [24]. We

use the carrier density $n_p \cong 10^{23}$ m^{-3} as reported for BFO film [13]. For the case of $t = 0.2$ mm, $d_o \cong (2\varepsilon_o\varepsilon_p U_o/qn_p)^{1/2}$ was estimated to be ~330 nm, which is consistent with the depletion layer in ITO–BFO films [13]. The parameters C and U_o are related by the carrier charge q ($=CkT/U_o$), where we chose q as the electron charge $\sim 1.6 \times 10^{-19}$ C.

Finally, we consider three related questions. First, how do the shapes of our V_{oc} and J_{sc} curves versus I compare with those for other p–n-junction-based photovoltaic systems? Second, how can our model account for the similarities and differences between those systems and ours? Third, how does our model for these intensity dependences compare with other models?

Other reports [25, 26] show curves for V_{oc} versus I with convex shape similar to ours. However [25], shows linear dependence of J_{sc} on I, unlike our convex curves. Our model is able to account for this difference in J_{sc} behavior, by analyzing the differences in the ratios D_{oc} and D_{sc} shown in the insets of figures 3 and 4. Mathematically, from equations (12) and (16), one can think of F as being a function of D, and we find that $\partial F/\partial D > 0$ and so also $\partial D/\partial F > 0$. This means that $D_{sc} > D_{oc}$. The crucial factor in $F \equiv U_o/R_A J_{to}$ is the area-specific source resistance R_A. As R_A becomes infinite, D_{sc} and D_{oc} become equal. If $R_A = 0$, $D_{sc} = 1$. Physically, this means that there is no hindrance for photo-generated electron–hole pairs to travel around the circuit until they recombine, whereas for nonzero R_A this hindrance narrows the depletion-region width. For R_A small but nonzero, the parameter $1 - D_{sc}^2$ becomes small. If we expand equation (15) in this small parameter, we arrive at the relation

$$J_{sc} \text{ (small } R_A) \cong J_{to}\alpha I. \tag{17}$$

This relation that is linear in I can account for the linear dependence of J_{sc} on I observed by Cusano [25] if R_A is small.

Cusano [25] has no expressions for V_{oc} or J_{sc}. Rose [26] does not provide an expression for J_{sc}. Reference [26] shows a linear dependence in V_{oc} at low intensity, followed by a convex curve that saturates into a horizontal line. If we take the low and high intensity limits for D_{oc} in equation (12) and insert these values into equation (13), we obtain

$$\begin{aligned} V_{oc} \text{ (low } I) &\cong \alpha U_o I/(C + 1/2); \\ V_{oc} \text{ (high } I) &\cong U_o. \end{aligned} \tag{18}$$

Accordingly, our model predicts the same linear, convex curve, constant I dependence sequence that is presented by Rose [26].

4. Conclusions

The ITO film/BFO ceramic/Au film configuration exhibits significant photovoltaic effects under illumination of $\lambda =$ 405 nm, which strongly depend on light wavelength, illumination intensity, and thickness. The proposed model which includes both thermally generated and photo-excited electron–hole pairs, can reasonably describe the photovoltaic responses as a function of illumination intensity. This physical model can be applied to the photovoltaic effects in p–n junction type BFO thin films and pother systems.

Acknowledgment

This work was supported by National Science Council of Taiwan Grant No. 100-2112-M-030-002-MY3.

References

[1] Choi T, Lee S, Choi Y J, Kiryukhin V and Cheong S W 2009 *Science* **324** 63
[2] Ji W, Yao K and Liang Y C 2010 *Adv. Mater.* **22** 1763
[3] Spaldin N A, Cheong S W and Ramesh R 2010 *Phys. Today* **63** 38
[4] Himcinschi C, Vrejoiu I, Friedrich M, Nikulina E, Ding L, Cobet C, Esser N, Alexe M, Rafaja D and Zahn D R T 2010 *J. Appl. Phys.* **107** 123524
[5] Chen B, Li M, Liu Y, Zuo Z, Zhuge F, Zhan Q F and Li R W 2011 *Nanotechnology* **22** 195201
[6] Zang Y *et al* 2011 *Appl. Phys. Lett.* **99** 132904
[7] Ji W, Yao K and Liang Y C 2011 *Phys. Rev.* B **84** 094115
[8] Yang S Y *et al* 2010 *Nature Nanotechnol.* **5** 143
[9] Yi H T, Choi T, Choi S G, Oh Y S and Cheong S W 2011 *Adv. Mater.* **23** 3403
[10] Chen Y B, Katz M B, Pan X Q, Das R R, Kim D M, Baek S H and Eom C B 2007 *Appl. Phys. Lett.* **90** 072907
[11] Kundys B, Viret M, Colson D and Kundys D O 2010 *Nature Mater.* **9** 803
[12] Ihlefeld J F *et al* 2008 *Appl. Phys. Lett.* **92** 142908
[13] Yang S Y *et al* 2009 *Appl. Phys. Lett.* **95** 062909
[14] Glass A M, von der Linde L D and Negran T J 1974 *Appl. Phys. Lett.* **25** 233
[15] Kim H, Gilmore C M, Piqué A, Horwitz J S, Mattoussi H, Murata H, Kafafi Z H and Chrisey D B 1999 *J. Appl. Phys.* **86** 6451
[16] Rottmann M and Heckner K H 1995 *J. Phys. D: Appl. Phys.* **28** 1448
[17] Fujioka J, Nakamura M, Kawasaki M and Tokura Y 2012 *J. Appl. Phys.* **111** 016107
[18] Poosanaas P, Dogan A, Thakoor S and Uchino K 1998 *J. Appl. Phys.* **84** 1508
[19] Uchino K, Poosanaas P and Tonooka K 2001 *Ferroelectrics* **264** 303
[20] Takagi K, Kikuchi S and Li J F 2004 *J. Am. Ceram. Soc.* **87** 1477
[21] Tu C S, Wang F T, Chien R R, Schmidt V H, Hung T M and Tseng C T 2006 *Appl. Phys. Lett.* **88** 032902
[22] Qin M, Yao K and Liang Y C 2009 *Appl. Phys. Lett.* **95** 022912
[23] Shockley W and Queisser H J 1961 *J. Appl. Phys.* **32** 510
[24] Tu C S, Yang W C, Schmidt V H and Chien R R 2011 *J. Appl. Phys.* **110** 114114
[25] Cusano D A 1963 *Solid-State Electron.* **6** 217
[26] Rose A 1960 *J. Appl. Phys.* **31** 1640